Axionic and Phonon Polaritons for Axion Dark Matter Detection

Jan Schütte-Engel

PNU-IBS workshop on Axion Physics: Search for axions, Haeundae, Busan, South Korea, 07/12/23

[**JSE**, D.J.E. Marsh, A.J. Millar, et al. 21], [D. J. E. Marsh, K.C. Fong, E. Lentz, L. Smejkal, M. Ali, 18] [D.J.E. Marsh, J.I. McDonald, A.J. Millar, **JSE** 22]

Berkeley UNIVERSITY OF CALIFORNIA

RIKEN

Constraints on Dark Matter axions

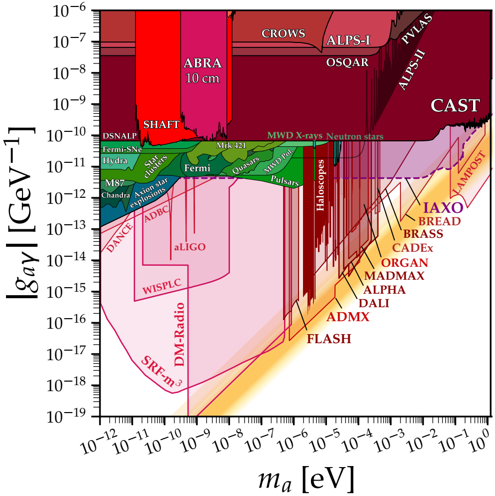

adapted from [cajohare.github.io/AxionLimits/]

Constraints on Dark Matter axions

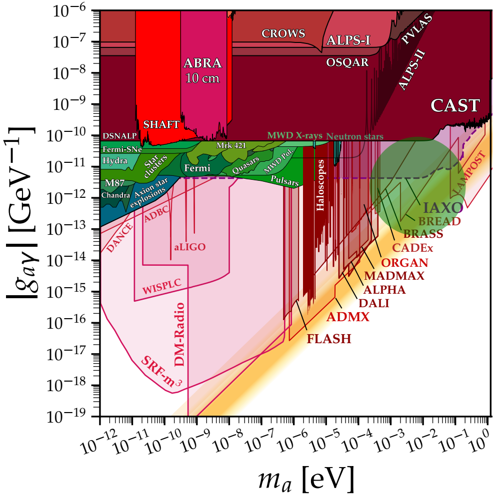

adapted from [cajohare.github.io/AxionLimits/]

Axion DM Detection with

Axion quasiparticles

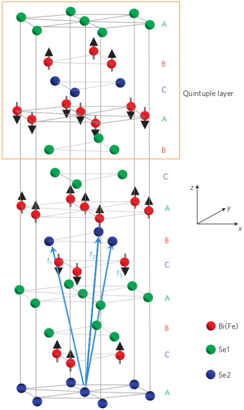

[Li, Wang, Qi, Zhang 10]

Phonons

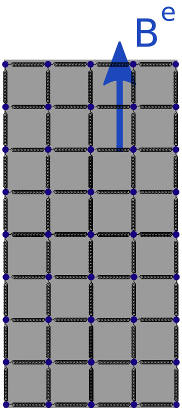

Axion Quasiparticles (AQs)

Axion Quasiparticles (AQs)

arise in materials with $\mathcal{L} \supset \delta\Theta \boldsymbol{E} \cdot \boldsymbol{B}$

Topological insulator in a nutshell

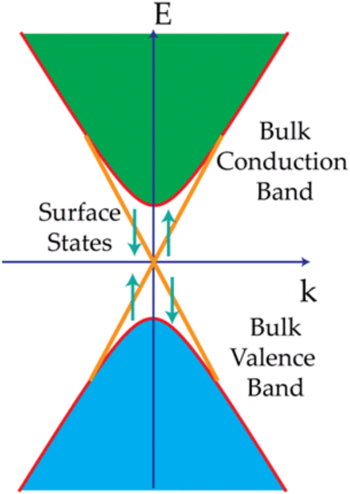

[hoffman.physics.harvard]

- Topological insulator is insulating in the bulk and conducting on the surface
- Physical realization for example: Bi_2Te_3 or Bi_2Se_3

Effective description of topological insulator

- Topological insulator

$$S_{TI} = \int d^3x dt (\epsilon E^2 - \frac{1}{\mu} B^2) + \underbrace{\frac{\theta}{2\pi} \frac{\alpha}{2\pi} \int d^3x dt \boldsymbol{E} \cdot \boldsymbol{B}}_{S_\theta}$$

- θ is periodic in 2π

$$\theta \boldsymbol{E} \cdot \boldsymbol{B} \overset{T}{\rightarrow} -\theta \boldsymbol{E} \cdot \boldsymbol{B} \overset{\theta \text{ periodic}}{\rightarrow} (-\theta + 2\pi) \boldsymbol{E} \cdot \boldsymbol{B} \overset{\text{T inv.}}{\Rightarrow} \theta = \pi$$

- Time reversal invariant insulator $\theta = 0, \pi$ ($\theta = 0$ normal insulator, $\theta = \pi$ topological insulator)
- Most topological insulators have T symmetry.

Dynamical Axion field in Topological Magnetic Insulator

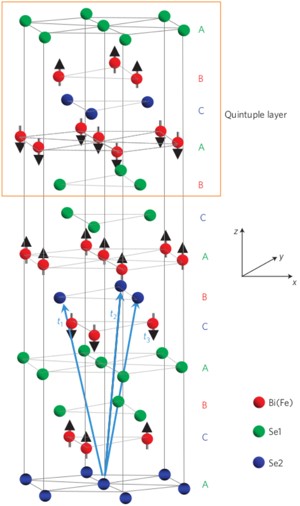

[Li, Wang, Qi, Zhang 10]

- Add P or T breaking terms $\Rightarrow \theta$ deviates form 0, π, realization in antiferromagnetic phase
- Antiferromagnetic phase has spin wave excitations (Magnons) which behave as a dynamical axion field
- Suggested material: $(Bi_{1-x}Fe_x)_2Se_3$

Dynamical AQs in antiferromagnets

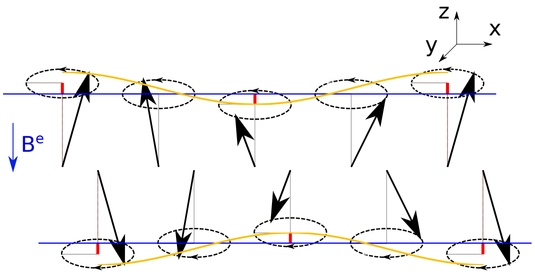

Néel vector $\boldsymbol{M}^- = \frac{1}{2}\left(\langle \boldsymbol{S}_A \rangle - \langle \boldsymbol{S}_B \rangle\right)$

AQ is longitudinal spin wave

$$\delta\Theta(\boldsymbol{x}, t) = \delta M_z^-(\boldsymbol{x}, t)$$
$$\mathcal{L} \supset \frac{\alpha}{4\pi^2} \delta\Theta \boldsymbol{E} \cdot \boldsymbol{B}$$

[Li, Wang, Qi, Zhang 10], [Affleк 89]

Other suggested material candidates

- $Mn_2Bi_2Te_5$ [Cao, Han, et al. 21]
- Weyl semimetal [J. Gooth, B. Bradlyn et al. 19]
- topological paramagnetic insulator [Wang, Lian, Zhang, 16]

Detecting Axion Quasiparticles

$$\begin{aligned}
\nabla \cdot \boldsymbol{D} &= -\frac{\alpha}{\pi} \nabla \Theta \cdot \boldsymbol{B}^e, \\
\nabla \times \boldsymbol{H} - \partial_t \boldsymbol{D} &= \frac{\alpha}{\pi} \boldsymbol{B}^e \partial_t \Theta, \\
\partial_t^2 \delta\Theta + m_\Theta^2 \delta\Theta &= \frac{1}{f_\Theta^2} \frac{\alpha}{\pi} \boldsymbol{E} \cdot \boldsymbol{B}^e.
\end{aligned}$$

with $\boldsymbol{D} = n^2 \boldsymbol{E}, \boldsymbol{H} = \boldsymbol{B}$ and $\Theta \equiv \delta\Theta + \Theta^0$

Axion polariton dispersion relation

Mixing of AQ with photons $\Rightarrow$ axion polariton (collective mode is coupled linearly to photons)

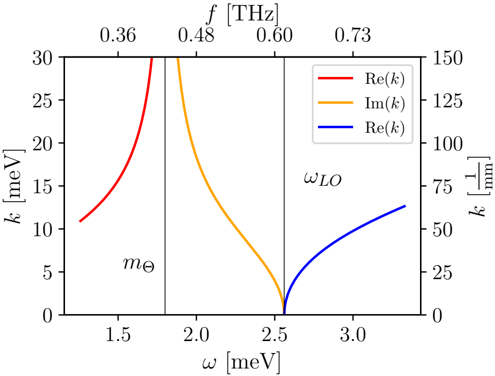

$$k^2 = n_\Theta^2 \omega^2$$

$$n_\Theta^2 = n^2 \left[\frac{b^2}{m_\Theta^2 - \omega^2} + 1 \right]$$

$$m_\Theta = 2\,\mathrm{meV}$$

$$\omega_{\mathrm{LO}} = \sqrt{m_\Theta^2 + b^2}$$

$$b = \frac{\alpha}{\pi\sqrt{2}} \frac{B^e}{n f_\Theta} = 1.6\,\mathrm{meV} \left(\frac{25}{n^2} \right)^{1/2} \left(\frac{B^e}{2\,\mathrm{T}} \right) \left(\frac{70\,\mathrm{eV}}{f_\Theta} \right) .$$

Detecting Axion Quasiparticles

THz time domain spectroscopy

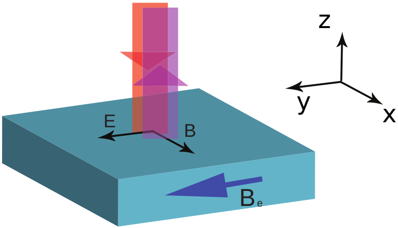

[Li, Wang, Qi, Zhang 10]

In the medium:

$$E(z) = C_+ e^{i\omega n_\theta z} + C_- e^{-i\omega n_\theta z}$$
$$\delta\Theta(z) = D_+ e^{i\omega n_\theta z} + D_- e^{-i\omega n_\theta z}$$

Boundary conditions:

$$\begin{aligned} \hat{\boldsymbol{e}}_z \cdot (\boldsymbol{D}_{\text{vac}} - \boldsymbol{D}_{\text{mat}}) &= 0, \\ \hat{\boldsymbol{e}}_z \times (\boldsymbol{H}_{\text{vac}} - \boldsymbol{H}_{\text{mat}}) &= 0. \end{aligned}$$

Detecting Axion Quasiparticles

THz time domain spectroscopy

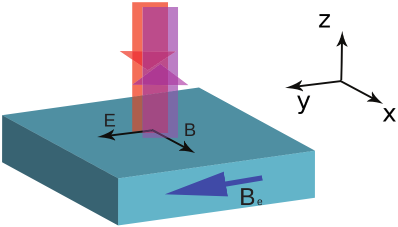

[Li, Wang, Qi, Zhang 10]

In the medium:

$$E(z) = C_+ e^{i\omega n_\theta z} + C_- e^{-i\omega n_\theta z}$$
$$\delta\Theta(z) = D_+ e^{i\omega n_\theta z} + D_- e^{-i\omega n_\theta z}$$

Boundary conditions:

$$\hat{\boldsymbol{e}}_z \cdot (\boldsymbol{D}_{\text{vac}} - \boldsymbol{D}_{\text{mat}}) = 0,$$
$$\hat{\boldsymbol{e}}_z \times (\boldsymbol{H}_{\text{vac}} - \boldsymbol{H}_{\text{mat}}) = 0.$$

Short aside:

$$\nabla \cdot \boldsymbol{D} = -\frac{\alpha}{\pi} \nabla\Theta \cdot \boldsymbol{B},$$
$$\nabla \times \boldsymbol{H} - \partial_t \boldsymbol{D} = \frac{\alpha}{\pi} \left(\boldsymbol{B} \partial_t \Theta - \boldsymbol{E} \times \nabla\Theta \right),$$

Detecting Axion Quasiparticles

THz time domain spectroscopy

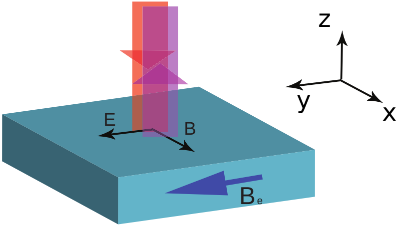

[Li, Wang, Qi, Zhang 10]

In the medium:

$$E(z) = C_+ e^{i\omega n_\theta z} + C_- e^{-i\omega n_\theta z}$$
$$\delta\Theta(z) = D_+ e^{i\omega n_\theta z} + D_- e^{-i\omega n_\theta z}$$

Boundary conditions:

$$\begin{aligned} \hat{\boldsymbol{e}}_z \cdot (\boldsymbol{D}_{\text{vac}} - \boldsymbol{D}_{\text{mat}}) &= 0, \\ \hat{\boldsymbol{e}}_z \times (\boldsymbol{H}_{\text{vac}} - \boldsymbol{H}_{\text{mat}}) &= 0. \end{aligned}$$

Short aside:

$$\begin{aligned} \nabla \cdot \boldsymbol{D}_\Theta &= 0 \\ \nabla \times \boldsymbol{H}_\Theta - \partial_t \boldsymbol{D}_\Theta &= 0, \end{aligned}$$

Detecting Axion Quasiparticles

THz time domain spectroscopy

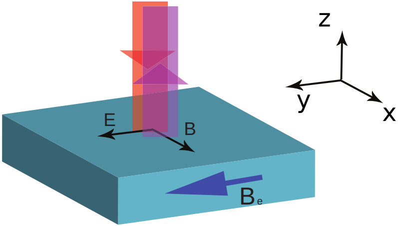

[Li, Wang, Qi, Zhang 10]

In the medium:

$$E(z) = C_+ e^{i\omega n_\theta z} + C_- e^{-i\omega n_\theta z}$$
$$\delta\Theta(z) = D_+ e^{i\omega n_\theta z} + D_- e^{-i\omega n_\theta z}$$

Boundary conditions:

$$\hat{\boldsymbol{e}}_z \cdot (\boldsymbol{D}_{\mathrm{vac}} - \boldsymbol{D}_{\mathrm{mat}}) = 0,$$
$$\hat{\boldsymbol{e}}_z \times (\boldsymbol{H}_{\mathrm{vac}} - \boldsymbol{H}_{\mathrm{mat}}) = 0.$$

Short aside:

$$\boldsymbol{n} \cdot (\boldsymbol{D}_{\Theta,\mathrm{vac}} - \boldsymbol{D}_{\Theta,\mathrm{mat}}) = 0$$
$$\boldsymbol{n} \times (\boldsymbol{H}_{\Theta,\mathrm{vac}} - \boldsymbol{H}_{\Theta,\mathrm{mat}}) = 0$$

where $\boldsymbol{D}_\Theta = \boldsymbol{D} + \frac{\alpha}{\pi}\Theta\boldsymbol{B}$, $\boldsymbol{H}_\Theta = \boldsymbol{H} - \frac{\alpha}{\pi}\Theta\boldsymbol{E}$.

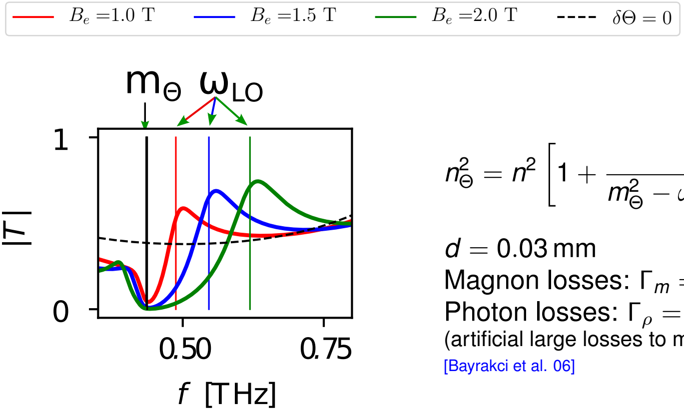

$$n_\Theta^2 = n^2 \left[1 + \frac{b^2}{m_\Theta^2 - \omega^2 - i\Gamma_m \omega} + i\frac{\Gamma_\rho}{\omega} \right]$$

$d = 0.03\,\text{mm}$
Magnon losses: $\Gamma_m = 10^{-1}$
Photon losses: $\Gamma_\rho = 10^{-1}$
(artificial large losses to make effect clearer.)
[Bayrakci et al. 06]

$$T = \frac{2in_\Theta}{\left(n_\Theta^2 + 1\right)\sin\Delta + 2in_\Theta \cos\Delta} + \mathcal{O}\left(\left(\frac{\alpha}{\pi}\Theta^0\right)^2\right)$$

with $\Delta = dk_\Theta$

Axion dark matter detection with AQs

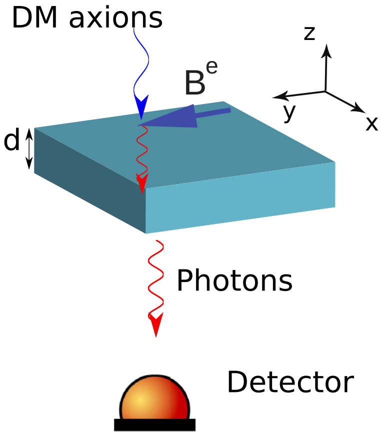

Surface Area $A = (20\,\mathrm{cm})^2$

TOORAD (Topological Resonant Axion Detection)

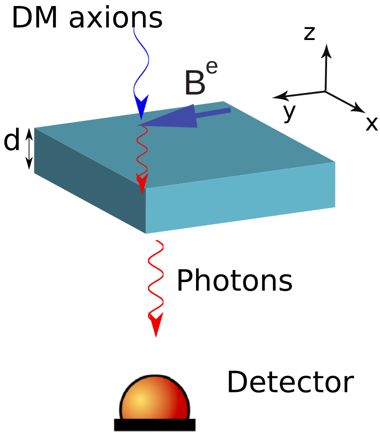

Surface Area $A = (20\,\mathrm{cm})^2$

TOORAD (Topological Resonant Axion Detection)

$$
\begin{aligned}
\nabla\cdot\boldsymbol{D} &= -\frac{\alpha}{\pi}\nabla\Theta\cdot\boldsymbol{B}^e \\
&\quad -g_{a\gamma}\nabla a\cdot\boldsymbol{B}^e, \\
\nabla\times\boldsymbol{H}-\partial_t\boldsymbol{D} &= \frac{\alpha}{\pi}\boldsymbol{B}^e\partial_t\Theta \\
&\quad +g_{a\gamma}\boldsymbol{B}^e\partial_t a, \\
\nabla\cdot\boldsymbol{B} &= 0, \\
\nabla\times\boldsymbol{E}+\partial_t\boldsymbol{B} &= 0, \\
\partial_t^2\delta\Theta + m_\Theta^2\delta\Theta &= \frac{1}{f_\Theta^2}\frac{\alpha}{\pi}\boldsymbol{E}\cdot\boldsymbol{B}^e, \\
(\partial_t^2-\nabla^2+m_a^2)a &= g_{a\gamma}\boldsymbol{E}\cdot\boldsymbol{B}^e.
\end{aligned}
$$

Effective description: axion induced E-field excites material with effective refraction index n_Θ

$$\partial_z^2 E(z) + \omega^2 n_\Theta^2(\omega) E(z) = -\omega^2 E_a$$

Physical understanding

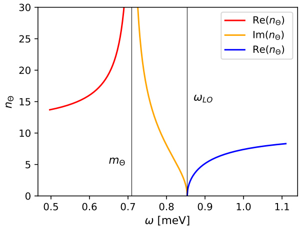

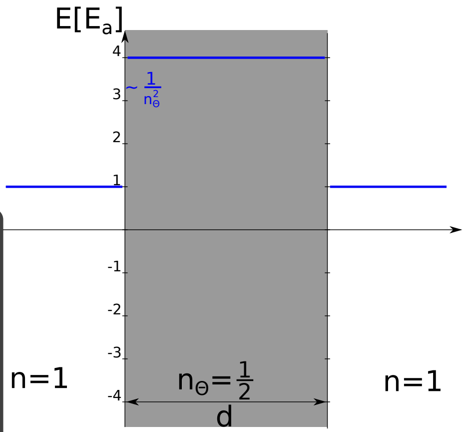

Resonance condition:

$$\pi = n_\Theta(\omega_{\rm res})\omega_{\rm res} d$$

$$n_\Theta(\omega) = n\left[\frac{b^2}{m_\Theta^2 - \omega^2} + 1\right]^{\frac{1}{2}}$$

$$b \sim \text{ext. B-field}$$

Principle similar to dielectric haloscopes. Matching *E* and *B*-fields at interfaces. Similarities to Fabry-Perot cavity.

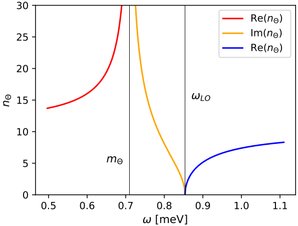

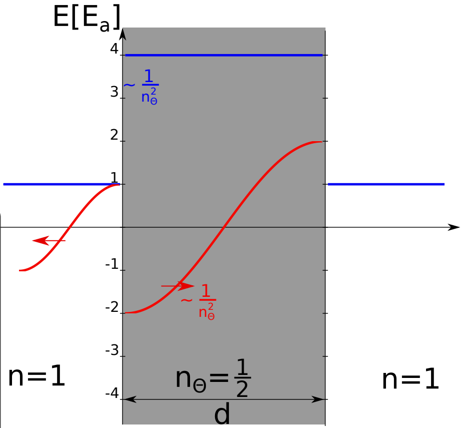

Resonance condition:

$$\pi = n_\Theta(\omega_{\text{res}})\omega_{\text{res}} d$$

$$n_\Theta(\omega) = n\left[\frac{b^2}{m_\Theta^2 - \omega^2} + 1\right]^{\frac{1}{2}}$$

$$b \sim \text{ext. B-field}$$

Principle similar to dielectric haloscopes. Matching *E* and *B*-fields at interfaces.
Similarities to Fabry-Perot cavity.

Physical understanding

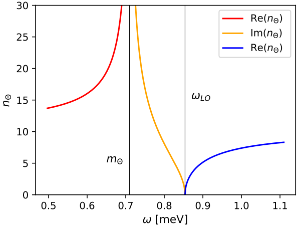

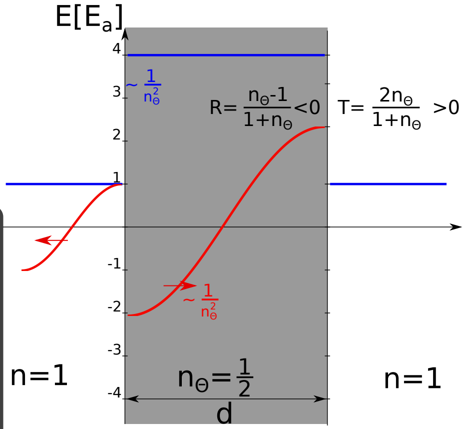

Resonance condition:

$$\pi = n_\Theta(\omega_{\text{res}})\omega_{\text{res}} d$$

$$n_\Theta(\omega) = n\left[\frac{b^2}{m_\Theta^2 - \omega^2} + 1\right]^{\frac{1}{2}}$$

$$b \sim \text{ext. B-field}$$

Principle similar to dielectric haloscopes. Matching *E* and *B*-fields at interfaces.
Similarities to Fabry-Perot cavity.

Physical understanding

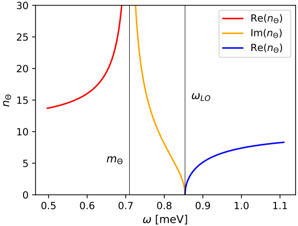

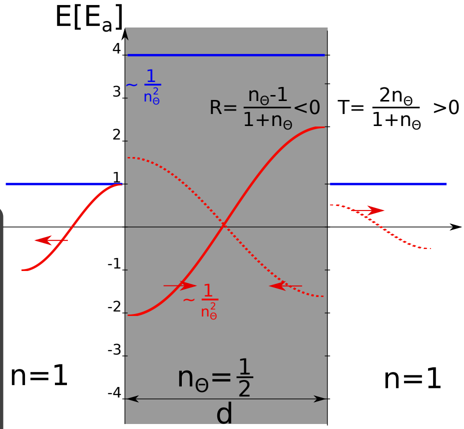

Resonance condition:

$$\pi = n_\Theta(\omega_{\rm res})\omega_{\rm res} d$$

$$n_\Theta(\omega) = n\left[\frac{b^2}{m_\Theta^2 - \omega^2} + 1\right]^{\frac{1}{2}}$$

$$b \sim \text{ext. B-field}$$

Principle similar to dielectric haloscopes. Matching *E* and *B*-fields at interfaces.
Similarities to Fabry-Perot cavity.

Physical understanding

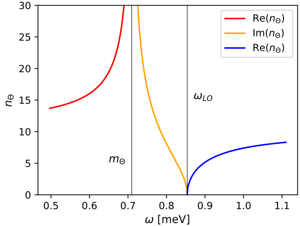

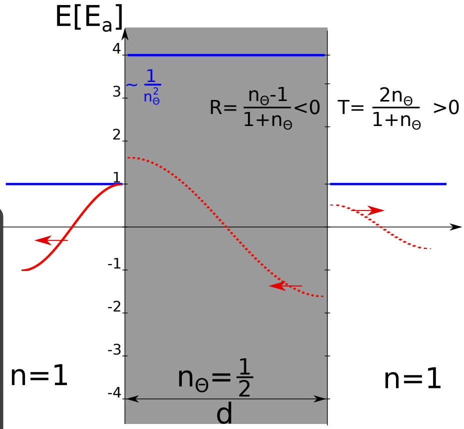

Resonance condition:

$$\pi = n_\Theta(\omega_{\rm res})\omega_{\rm res} d$$

$$n_\Theta(\omega) = n\left[\frac{b^2}{m_\Theta^2 - \omega^2} + 1\right]^{\frac{1}{2}}$$

$$b \sim \text{ext. B-field}$$

Principle similar to dielectric haloscopes. Matching *E* and *B*-fields at interfaces.
Similarities to Fabry-Perot cavity.

Physical understanding

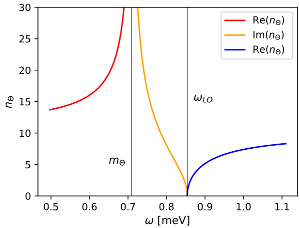

Resonance condition:

$$\pi = n_\Theta(\omega_{\rm res})\omega_{\rm res} d$$

$$n_\Theta(\omega) = n\left[\frac{b^2}{m_\Theta^2 - \omega^2} + 1\right]^{\frac{1}{2}}$$

$$b \sim \text{ext. B-field}$$

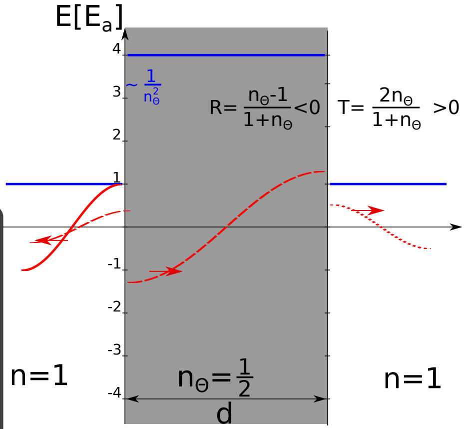

Principle similar to dielectric haloscopes. Matching E and B-fields at interfaces.
Similarities to Fabry-Perot cavity.

Physical understanding

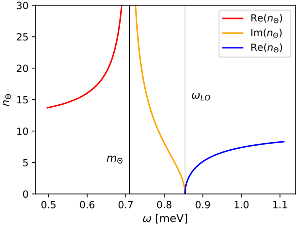

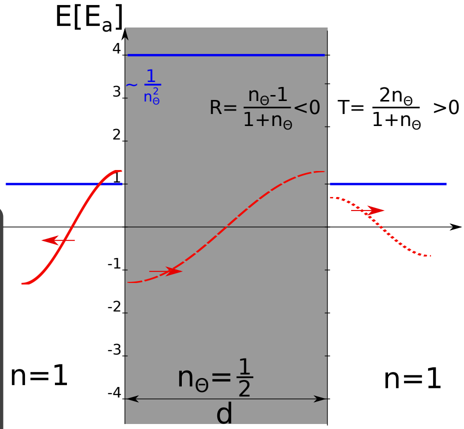

Resonance condition:

$$\pi = n_\Theta(\omega_{\rm res})\omega_{\rm res} d$$

$$n_\Theta(\omega) = n\left[\frac{b^2}{m_\Theta^2 - \omega^2} + 1\right]^{\frac{1}{2}}$$

$$b \sim \text{ext. B-field}$$

Principle similar to dielectric haloscopes. Matching E and B-fields at interfaces.
Similarities to Fabry-Perot cavity.

Physical understanding

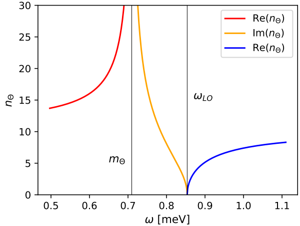

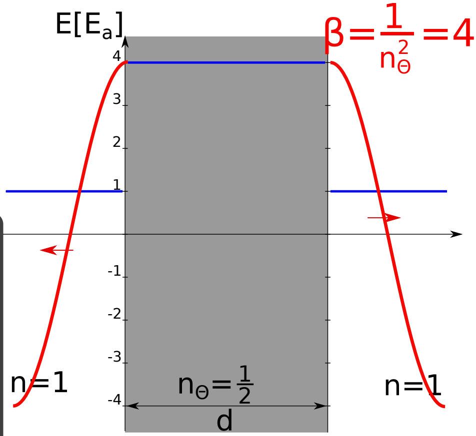

Resonance condition:

$$\begin{aligned} \pi &= n_\Theta(\omega_{\text{res}})\omega_{\text{res}} d \\ n_\Theta(\omega) &= n\left[\frac{b^2}{m_\Theta^2 - \omega^2} + 1\right]^{\frac{1}{2}} \\ b &\sim \text{ext. B-field} \end{aligned}$$

Principle similar to dielectric haloscopes. Matching *E* and *B*-fields at interfaces.
Similarities to Fabry-Perot cavity.

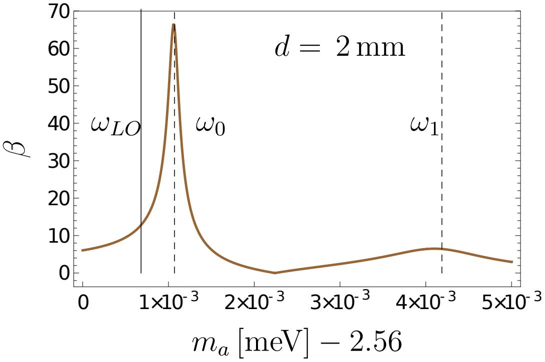

External *B*-field fixed in figure. Changing it shifts resonance peaks $\Rightarrow$ scan different axion masses.

$$\beta = \frac{E_{\text{out}}}{E_a}$$

$$\beta = \frac{\sin(\Delta/2)\left(1 - n_\Theta^2\right)}{n_\Theta\left(n_\Theta \sin(\Delta/2) + i\cos(\Delta/2)\right)}$$

Resonance condition:

$$\Delta = \Delta_j = n_\Theta(\omega_j)\omega_j d = (2j+1)\pi,\ j \in \mathbb{N}_0$$

Including losses

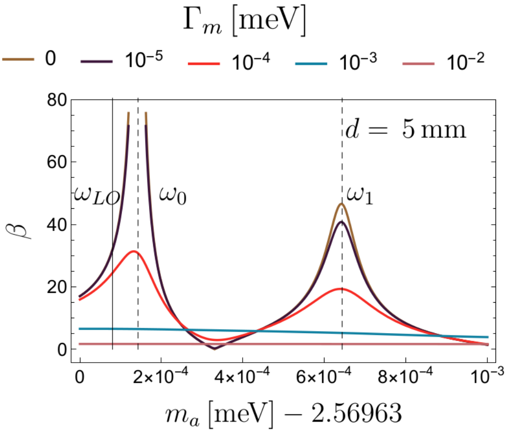

$$n_\Theta^2 = n^2 \left[1 + \frac{b^2}{m_\Theta^2 - \omega^2 - i\Gamma_m \omega} + i\frac{\Gamma_\rho}{\omega} \right]$$

$$\gamma_j = \frac{4b^2\Delta_j^2}{n^2\omega_{\mathrm{LO}}^4 d^3} + \left(\Gamma_m + \frac{b^2}{\omega_{\mathrm{LO}}^2}\Gamma_\rho \right)$$

$$\beta(\omega_j) = \frac{4b^2}{n^2\omega_{\mathrm{LO}}^2 d\gamma_j}$$

Optimal thickness

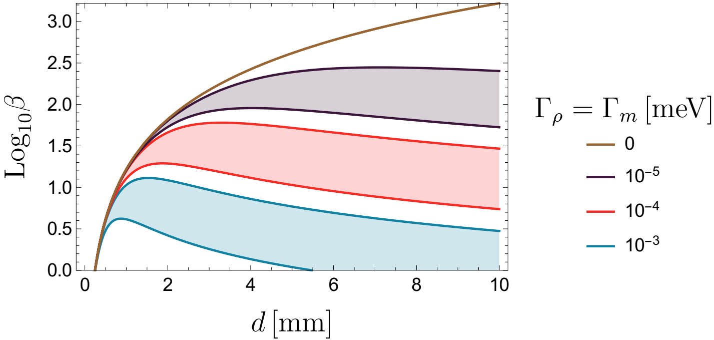

Bands indicate changing refractive index *n*.

$$d_{\mathrm{opt}} = \frac{2}{\omega_{\mathrm{LO}}}\left(\frac{\Delta_j}{n}\right)^{\frac{2}{3}}\left(\frac{1}{\frac{\Gamma_\rho}{\omega_{\mathrm{LO}}}+\frac{\Gamma_m\omega_{\mathrm{LO}}}{b^2}}\right)^{\frac{1}{3}}.$$

Single photon detection

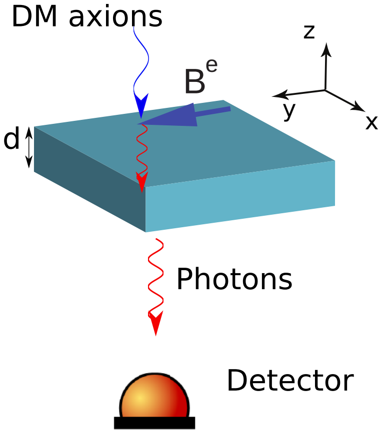

Number of signal events per time

$$\lambda_s = \eta \frac{|E_a|^2}{2\omega} \beta^2 A$$

η photon counting efficiency, A surface area, $E_0 = g_{a\gamma} B^e \frac{\sqrt{2\rho_a}}{m_a}$

Single photon counting

$$\lambda_s < \frac{1}{\tau} + 2\sqrt{\frac{\lambda_d}{\tau}}$$

[Bityukov,Krasnikov, 98]

λ_d dark count rate, τ measurement time.

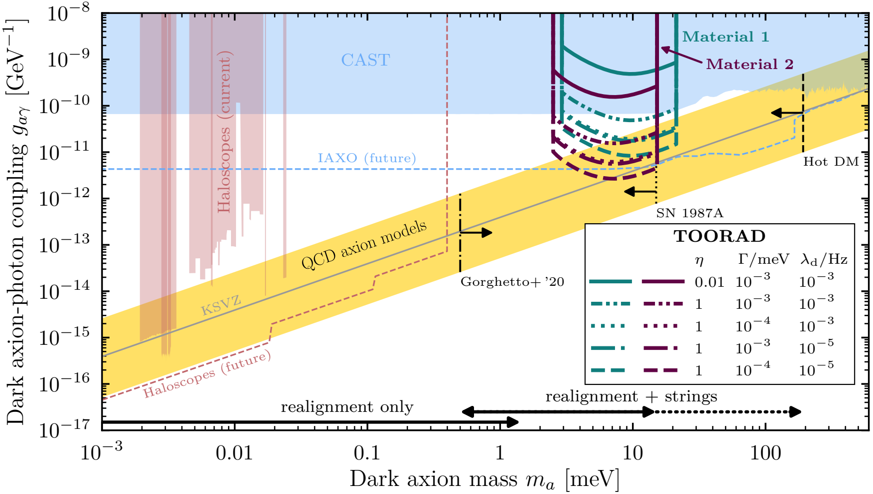

Material 1: $Bi_{1-x}Fe_xSe_3$, Material 2: $Mn_2Bi_2Te_5$

values fo the detector parameters: [Fong and Schwab 12], [Hocherg et al. 19]

Axion DM detection with phonon polaritons

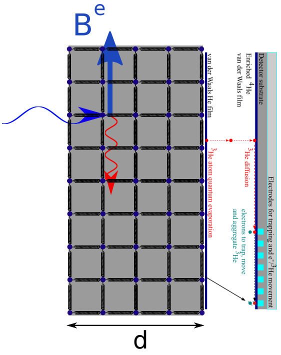

[A. Mitridate, T. Trickle, Z. Zhang, K.M. Zurek, 20]
example for single phonon readout scheme [S. A. Lyon et al. arxiv:2201.00738].

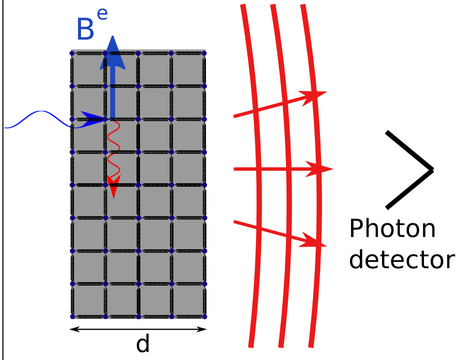

[D.J.E. Marsh, J.I. McDonald, A.J. Millar, **JSE** 22]

Effective description

$$n^2(\omega) = \epsilon_\infty \left(1 + \frac{\omega_{\mathrm{pl}}^2/\epsilon_\infty}{\omega_{\mathrm{TO}}^2 - \omega^2 - i\omega\Gamma} + i\frac{\Gamma_\rho}{\omega}\right) .$$

compare to

$$n_\Theta^2 = n^2 \left[1 + \frac{b^2}{m_\Theta^2 - \omega^2 - i\Gamma_m\omega} + i\frac{\Gamma_\rho}{\omega}\right]$$

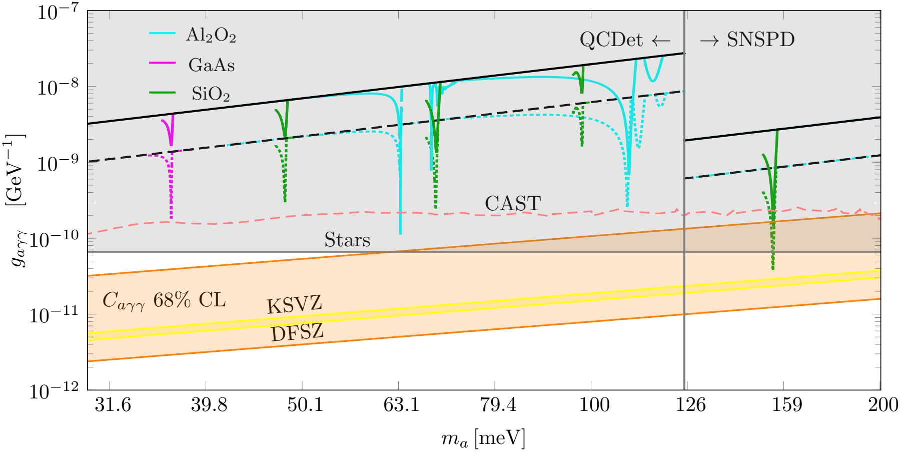

black: dish antenna, integration time one month per resonance, $A = (0.1\mathrm{m})^2$, more optimistic dashed (100 ties better dark count rate) and losses dominated by impurities.

High frequency Gravitational wave detection

GW photon mixing

$$\mathcal{L} \supset -\frac{1}{4}\eta^{\mu\alpha}\eta^{\nu\beta}F_{\mu\nu}F_{\alpha\beta}$$

In curved spacetime:

$$\mathcal{L} \supset -\sqrt{-g}\,\frac{1}{4}g^{\mu\alpha}g^{\nu\beta}F_{\mu\nu}F_{\alpha\beta}$$

Linearized Gravity

$$g_{\mu\nu} = \eta_{\mu\nu} + h_{\mu\nu}$$

Then Lagrangian contains terms of the form:

$$\mathcal{L} \supset -\frac{1}{4}\eta^{\mu\alpha}\,h^{\nu\beta}\,F_{\mu\nu}F_{\alpha\beta}$$

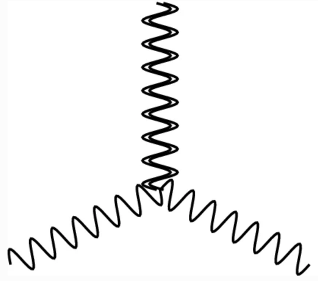

cf. axions $\mathcal{L} \supset -\frac{1}{4}g_{a\gamma}\,a\,F_{\mu\nu}\tilde{F}^{\mu\nu}$

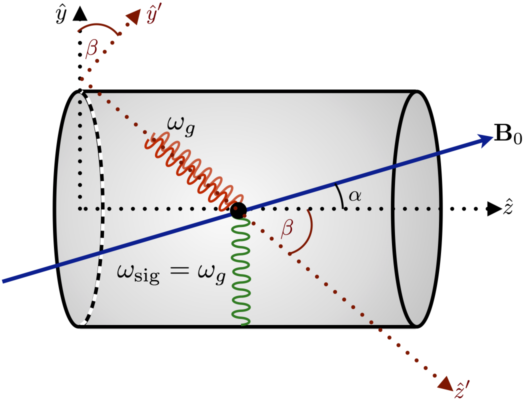

Signals can arise from

Mixing GW with photons

Movement of walls (free charges) in static external B-field induce a current

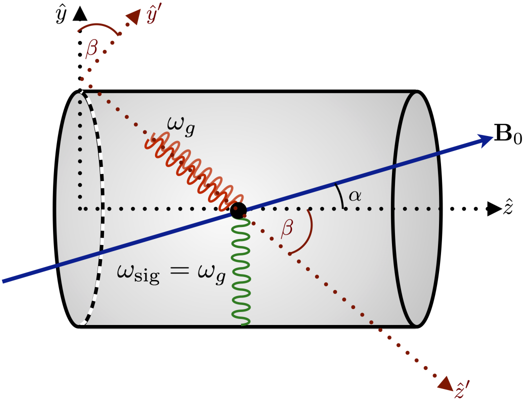

Signals can arise from

Mixing GW with photons

Movement of walls (free charges) in static external B-field induce a current

Signal in two benchmark scenarios

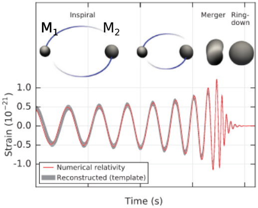

- Keep cavity fixed
- Sweep through all cavity modes

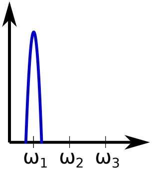

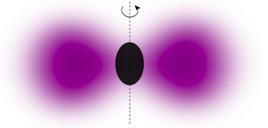

- Change cavity to scan different resonance frequencies
- GW frequency from superradiant cloud fixed

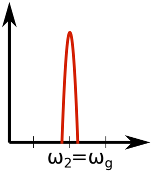

Signal in two benchmark scenarios

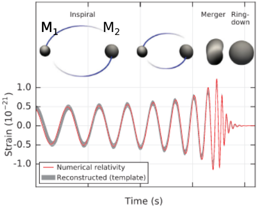

- Keep cavity fixed
- Sweep through all cavity modes

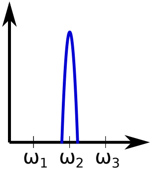

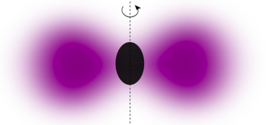

- Change cavity to scan different resonance frequencies
- GW frequency from superradiant cloud fixed

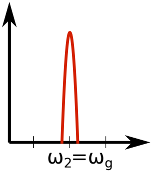

Signal in two benchmark scenarios

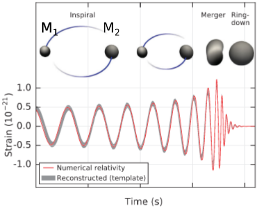

- Keep cavity fixed
- Sweep through all cavity modes

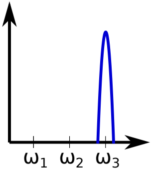

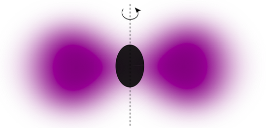

- Change cavity to scan different resonance frequencies
- GW frequency from superradiant cloud fixed

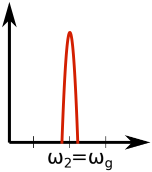

Sensitivity estimate

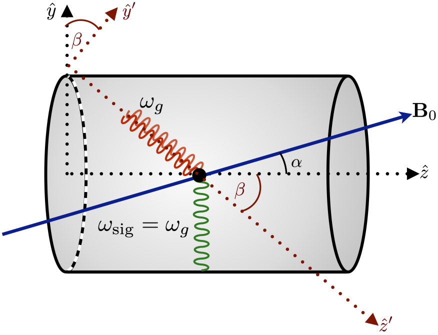

$$\text{SNR} \simeq \frac{P_{\text{sig}}}{T_{\text{sys}}} \sqrt{\frac{t_{\text{int}}}{\Delta\nu}}$$

$$h_0 \gtrsim 3 \times 10^{-22} \times \left(\frac{1\ \text{GHz}}{\omega_g/2\pi}\right)^{3/2} \left(\frac{0.1}{\eta_n}\right) \left(\frac{8\ \text{T}}{B_0}\right) \left(\frac{0.1\ \text{m}^3}{V_{\text{cav}}}\right)^{5/6} \times$$

$$\times \left(\frac{10^5}{Q}\right)^{1/2} \left(\frac{T_{\text{sys}}}{1\ \text{K}}\right)^{1/2} \left(\frac{\Delta\nu}{10\ \text{kHz}}\right)^{1/4} \left(\frac{1\ \text{min}}{t_{\text{int}}}\right)^{1/4}$$

Bandwidth $\Delta\nu = \frac{\omega_g}{2\pi Q}$.

Sensitivity of existing axion experiments

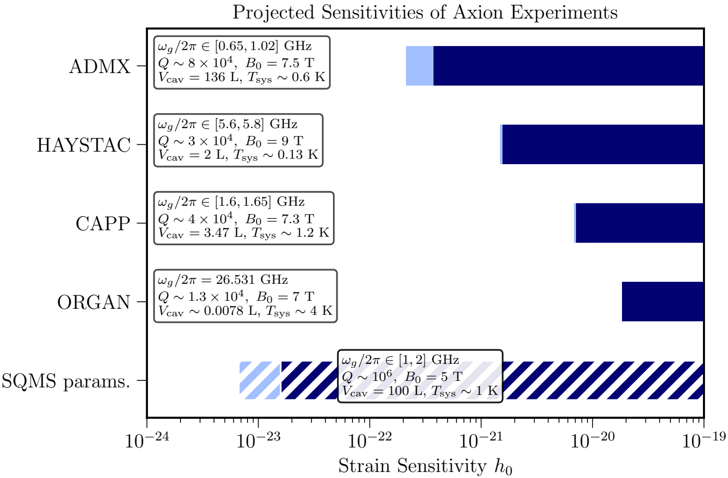

[A. Berlin, D. Blas, R. Tito D'Agnolo, S. A.R. Ellis, R. Harnik, Y. Kahn 21]

Existing axion experiments only need to reanalyze their data!

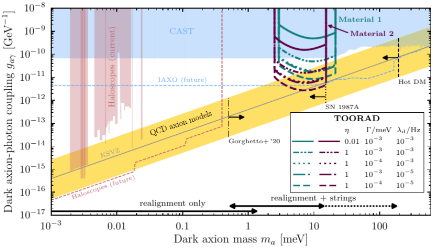

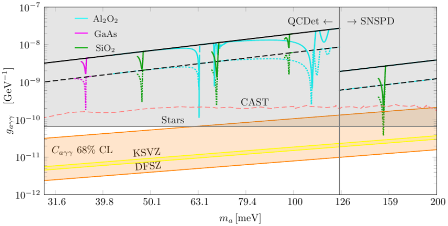

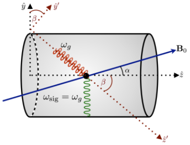

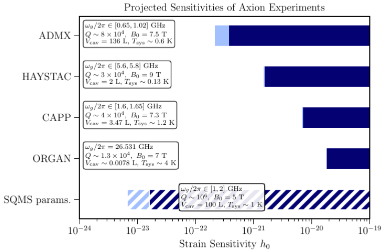

Thank you for your attention